

I. INTRODUCTION

Over the last two decades, the electron has proved to be a highly effective probe of the small-distance structure of the nucleon. As the electromagnetic interaction of the electron is explicitly calculable in quantum electrodynamics⁽¹⁾, electron-nucleon (e-N) scattering experiments can be unambiguously interpreted in terms of the structure of the probed nucleon. In the latter half of the 1950's the elastic electron-proton (e-p) and quasi-elastic electron-deuteron (e-d) scattering experiments of Hofstadter and collaborators⁽²⁾ indicated that the proton and neutron had finite sizes of order 10^{-13} cm. Electron-nucleon scattering experiments^(3,4) of the middle 1960's established that the nucleon form factors fell rapidly with increasing momentum transfer, suggesting a composite picture of the nucleon. In 1968, results from the first small-angle inelastic e-p scattering experiment⁽⁵⁾ at the Stanford Linear Accelerator Center (SLAC) suggested that the proton was composed of hypothetical pointlike constituents.⁽⁶⁾ The approximate scaling of the proton structure functions, verified by that experiment and a large-angle inelastic e-p experiment⁽⁷⁾ in the region of momentum and energy transfers significantly greater than the proton mass, provided the most straightforward and convincing evidence for this hypothesis. The large-angle experiments reported here repeat the earlier large-angle e-p experiment⁽⁷⁾ with improved statistical accuracy and expanded kinematic range;

inelastic e-d scattering is also measured for the first time over this expanded kinematic range. These experiments used the SLAC 8 GeV spectrometer and complement an earlier small-angle inelastic e-p and e-d scattering experiment⁽⁸⁾ done at SLAC. The data gathered in these experiments permit a detailed comparison of the inelastic electron-proton and electron-neutron (e-n) scattering cross sections. More stringent tests of structure function scaling are also facilitated by more complete and accurate data for the nucleon structure functions, as defined below.

In these experiments, an electron of incident energy E scatters from a nuclear target through a laboratory angle θ to a final energy E' , and only the electron is detected in the final state. In the first Born approximation, the scattering occurs through the exchange of a single virtual photon (Figure 1) of energy $\nu = E - E'$ and invariant momentum transfer $q^2 = -4EE' \sin^2 \theta / 2 = -Q^2$, where $\hbar = c = 1$ has been used and the mass of the electron has been neglected. The hadronic final state is unknown except for the invariant mass $W = (M^2 + 2M\nu - Q^2)^{1/2}$, where M is the proton mass. The differential cross section for electron scattering from the nuclear target is related to the two structure functions W_1 and W_2 according to⁽⁹⁾

$$\frac{d^2\sigma}{d\Omega dE'}(E, E', \theta) = \sigma_M \left\{ W_2(\nu, Q^2) + 2W_1(\nu, \theta') \tan^2 \frac{\theta}{2} \right\} \quad (\text{I.1})$$

where

$$\sigma_M = \frac{4\alpha^2 E'^2}{Q^4} \cos^2 \frac{\theta}{2}$$

is the Mott cross section, and $\alpha = e^2/4\pi = 1/137$. The structure

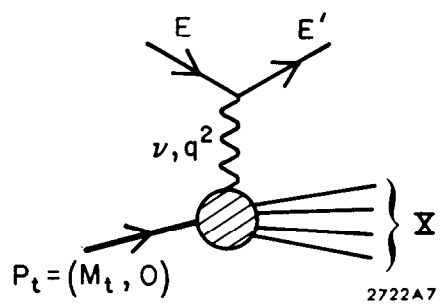


Fig. 1. Feynman diagram for inelastic electron-nucleon scattering in the first Born approximation.

functions W_1 and W_2 are similarly defined by equation (I.1) for the proton, deuteron, or neutron; they summarize all the information about the structure of these particles obtainable from unpolarized electron scattering.

Within the single-photon exchange approximation, one may alternatively view inelastic electron scattering as virtual photoproduction. Here, as opposed to photoproduction by real photons, the photon mass q^2 is variable and the exchanged photon may have a longitudinal as well as a transverse polarization. If the final state hadrons are not observed, the interference between these two components averages to zero, and the differential cross-section for inelastic electron scattering is related to the total cross sections for absorption of transverse, σ_T , and longitudinal, σ_L , virtual photons according to⁽¹⁰⁾

$$\frac{d^2\sigma}{d\Omega dE}(E, E', \theta) = \Gamma \left\{ \sigma_T(\nu, Q^2) + \epsilon \sigma_L(\nu, Q^2) \right\} \quad (I.2)$$

where

$$\Gamma = \frac{\alpha}{4\pi^2} \frac{KE'}{Q^2 E} \left(\frac{2}{1-\epsilon} \right) \quad , \quad \epsilon = \left\{ 1 + 2(1 + \nu^2/Q^2) \tan^2 \frac{\theta}{2} \right\}^{-1}$$

and

$$K = \frac{W^2 - M^2}{2M}$$

The quantity Γ is the flux of transverse virtual photons and ϵ is the degree of longitudinal polarization. Throughout this paper M and M_D are, respectively, the proton and deuteron masses. The cross sections σ_T and σ_L are related to the structure functions

$$\begin{aligned} W_1(\nu, Q^2) &= \frac{K}{4\pi^2\alpha} \sigma_T(\nu, Q^2) \\ W_2(\nu, Q^2) &= \frac{K}{4\pi^2\alpha} \left(\frac{Q^2}{Q^2 + \nu^2} \right) \left\{ \sigma_T(\nu, Q^2) + \sigma_L(\nu, Q^2) \right\} \end{aligned} \quad (I.3)$$

In the limit $Q^2 \rightarrow 0$, one obtains $\sigma_L \rightarrow 0$ and $\sigma_T \rightarrow \sigma_Y(\nu)$, where $\sigma_Y(\nu)$ the photoproduction cross section for real photons. The quantity R , defined as the ratio σ_L/σ_T , is related to the structure

functions by

$$R(\nu, Q^2) \equiv \frac{\sigma_L}{\sigma_T} = \frac{W_2}{W_1} \left(1 + \frac{\nu^2}{Q^2}\right) - 1 \quad (\text{I.4})$$

Equations (I.2) through (I.4) apply equally well for the proton, deuteron, or neutron.

A separate determination of the two inelastic structure functions W_1 and W_2 (or, equivalently, σ_L and σ_T) requires values of the differential cross section at several values of the angle θ for fixed ν and Q^2 . According to equation (I.2), σ_L is the slope and σ_T is the intercept of a linear fit to $\Sigma = \frac{1}{T} \frac{d^2\sigma}{d\Omega dE'}(\nu, Q^2, \theta)$. The structure functions W_1 and W_2 are then directly calculable from equation (I.3). Alternatively, one can extract W_1 and W_2 from a single differential cross section measurement by inserting a particular functional form for R in the equations

$$W_1 = \frac{1}{\sigma_M} \frac{d^2\sigma}{d\Omega dE'} \left\{ (1+R) \left(\frac{Q^2}{Q^2 + \nu^2} \right) + 2 \tan^2 \frac{\theta}{2} \right\}^{-1} \quad (\text{I.5})$$

$$W_2 = \frac{1}{\sigma_M} \frac{d^2\sigma}{d\Omega dE'} \left\{ 1 + \left(\frac{2}{1+R} \right) \left(\frac{Q^2 + \nu^2}{Q^2} \right) \tan^2 \frac{\theta}{2} \right\}^{-1}$$

The striking feature of the earlier inelastic e-p data^(5,7) was the scaling of the proton structure functions. Prior to those experiments, Bjorken had conjectured⁽¹¹⁾ that W_1 and W_2 might become functions of a single dimensionless variable x , i.e.,

$$2MW_1(\nu, Q^2) \Rightarrow F_1(x) \quad , \quad \nu W_2(\nu, Q^2) \Rightarrow F_2(x) \quad (\text{I.6})$$

in the limit $\nu \rightarrow \infty$ and $Q^2 \rightarrow \infty$, with $x = 1/\omega = Q^2/2M\nu$ held fixed. The earlier inelastic e-p experiments⁽⁷⁾ showed that approximate scaling behavior occurs at surprisingly non-asymptotic values of $Q^2 \geq 1.0 \text{ GeV}^2$ and $W \geq 2.6 \text{ GeV}$. This scaling behavior arises quite

naturally from a description of the proton in which the electron scatters from point-like, quasi-free constituents, or partons.⁽⁶⁾ In this simple parton model, x is the fraction of the proton's momentum carried by the struck parton in the infinite momentum frame, and $F_1(x)$ and $F_2(x)$ are unambiguously related to the parton charges and momentum distributions. A number of other models, including Regge-exchange models⁽¹²⁾, vector-meson dominance⁽¹³⁾, and s-channel resonance models⁽¹⁴⁾ can accommodate the observed scaling behavior for at least some range of x and Q^2 . Extended parton models^(15, 16) as well as conventional field theories⁽¹⁷⁾ and asymptotically free gauge theories⁽¹⁸⁾, predict small deviations from scaling that would have eluded the earlier inelastic e-p measurements. A more detailed and accurate examination of structure function scaling, which was one of the objectives of the experiments reported in this paper, can help to distinguish among these hypotheses.

A measurement of the deep inelastic e-n cross section also is a valuable test of the models that have been proposed to account for the observed scaling of the proton structure functions. Within parton models, predictions for the ratio of neutron to proton cross sections vary according to the assumptions about the parton charges and internal dynamics.⁽⁶⁾ A measurement of this ratio, which was the primary objective of these experiments, places constraints upon the possible parton models and other models of nucleon structure. Knowledge of both the neutron and proton cross

sections also allows a separate determination of the isovector and isoscalar contributions to the structure functions.

While unbound protons are readily available in liquid hydrogen targets, the simplest available target containing neutrons is deuterium, with a nuclear binding energy of 2.2 MeV. The extraction of neutron cross sections from inelastic e-p and e-d cross sections requires corrections for the effects of the binding of the nucleons in the deuteron. Corrections for the effects of Fermi motion of the nucleons are calculable in an impulse approximation. (19, 20) Measurement of inelastic e-p and e-d scattering at identical electron kinematics then permits the calculation of the neutron to proton cross section ratio

$$\sigma_n/\sigma_p = \left(\frac{d^2\sigma}{d\Omega dE'} \right)_n / \left(\frac{d^2\sigma}{d\Omega dE'} \right)_p \quad (\text{I.7})$$

Within parton models, the behavior of R as a function of Q^2 for fixed x reflects the spin quantum numbers of those charged partons carrying a fraction x of the nucleon's momentum. If the charged partons are purely spin 1/2, lightcone algebras predict that νR should scale. (6, 21, 22) For spin-0 partons R itself should scale. (23) The early inelastic e-p measurements (7) showed that R for the proton (R_p) was small and slowly varying, consistent with the constant value 0.18. Within a parton model the small values of R_p measured earlier favored predominantly spin 1/2 constituents. However, a convincing test of this hypothesis requires a detailed examination of the kinematic variation of R_p for fixed x. This examination and a comparison of R_p , R_d , and R_n

were among the objectives of these experiments.

In summary, a complete picture of the nucleon requires a measurement of the deep inelastic cross sections for both neutrons and protons. The ratio σ_n/σ_p provides important constraints upon parton models of the nucleon, while R yields information about the spin of the hypothetical constituents. In this paper we report the results of two experiments performed at SLAC in which both electron-proton and electron-deuteron cross sections were measured over wide ranges of E and E' for several scattering angles. Sections II - IV describe the experiments and the methods of analysis used to determine the inelastic e-p and e-d cross sections. Extraction of the inelastic e-n cross sections and the ratio σ_n/σ_p is described in Section V. The extraction of R from these cross sections is described in Section VI. Tests of structure function scaling are presented in Section VII, and Section VIII gives concluding remarks and discussion. Some early results of the two experiments were reported in several letters^(24, 25), and the first experiment is described in detail in two doctoral theses.^(20, 26)